Stochastic properties and Brillouin light scattering response of thermally driven collective magnonic modes on the arrays of dipole coupled nanostripes

M. P. Kostylev[1] and A. A. Stashkevich[2]
[1]*School of Physics–M013, University of Western Australia, 35 Stirling Highway, Crawley, Western Australia 6009, Australia*
[2]*LPMTM CNRS (UPR 9001), Université Paris 13, 93430 Villetaneuse, France*
(Received 15 October 2009; revised manuscript received 10 January 2010; published 16 February 2010)

In the present paper, the problem of thermal excitation of collective (magnonic) Bloch magnetostatic modes on a one-dimensional array of magnetic stripes has been addressed. It has been shown that partially phase-correlated oscillations localized on individual stripes can be regarded as an ensemble of individual harmonic oscillators interpretable in terms of independent degrees of freedom of the magnetic system subject to the low-energy Rayleigh-Jeans statistics. Numerical simulations of the Brillouin light scattering spectra, based on this approach, have shown that the *n*th Bloch mode in strongly coupled stripes contributes mainly to the scattering in the *n*th Brillouin zone. Our calculations have also confirmed numerically the noncoherent wide-angle character of the BLS, demonstrated experimentally earlier.

DOI: 10.1103/PhysRevB.81.054418 PACS number(s): 75.30.Ds, 78.35.+c

I. INTRODUCTION

From both fundamental and application viewpoints, magnetization dynamics in ferromagnetic media has become of utmost significance today. Rapid advances in spintronics during the last decade have contributed massively to the progress in this field. Suffice it to mention such discoveries as the giant magnetoresistance[1,2] and precessional switching applied to read-write processes in magnetic data storage.[3,4] In the case of relatively low-angle precession, magnetic dynamics manifests itself through magnetic excitations propagating in the bulk of such materials known as spin waves (SW), which are an object of great interest themselves. Historically, there are two different philosophies regarding this phenomenon from different points of view. It was with the incoherent SW driven by thermal agitation, better known as magnons, that the research in this domain began, as early as in the 1930s.[5] Since then such magnetic excitations, with a very short wavelength on the scale of the lattice parameter and hence entirely dominated by short-range exchange interactions, have become one of the fundamental notions in the solid-state physics of ferromagnetic media. Another view of the problem, seeing it from a completely different angle, is due to extensive application of ferrite materials to microwave components, beginning from the 1950s. In this case, the excitations, better known, as magnetostatic waves (MSW), are of long-wavelength nature, which is dictated by the macroscopic characteristic size of the microwave elements themselves. As a result, their behavior is completely described solely by the long-range dipole-dipole interactions (DDI). Further development of the latter concept in the 1960s was based on the breakthrough in the technology of single-crystal ferrite films, especially those based on yttrium iron garnet, with extremely low losses at microwave frequencies, suitable for effective signal processing, typically in delay lines in the frequency range from 2 to 20 GHz.[6] The coherent MSWs were excited by an external microwave source, i.e., by a special MSW antenna. The characteristic size of the ferrite films employed (their thickness) as well as that of the microstrip MSW antennas (their width) being in the micrometric range, the magnetic waves excited were of combined dipole-exchange nature.[7]

Extensive research in SW dynamics over the last few decades has lead to further merging of the two ideas thus leading to a generic concept of the dipole-exchange SW, either coherent or incoherent. One of the steps contributing to the reconciliation of the two points of view, especially important in the context of this paper, was due to the major improvements of the Brillouin light scattering (BLS) techniques, that took place in the late 1970s and early 1980s. While earlier setups, lacking in sensitivity, had to resort to generation of coherent SWs by external sources,[8,9] in the updated versions[10] preference was given to thermal magnons,[11] i.e., incoherent SWs. In spite of their low intensity, they ensured, owing to their thermal nature, excitation of modes with all possible wave numbers and temporal frequencies, within the range permitted by the SW spectra. The latter development spawned a series of papers providing adequate theoretical support for a newly emerged technique.[12,13] It relied on the modification of the fluctuation-dissipation theorem (FDT), developed somewhat earlier, for a magnetic system (see, for example, Refs. 14 and 15). The latter allows to relate the Fourier transform of the correlation function $\langle m_i(x',\vec{r},t)m_j(x,\vec{r}=0,t=0)\rangle$, determining the intensity of the light scattered at a given angle to the dynamic susceptibilities $g_{ij}(x,x',\vec{K},\omega\pm i\varepsilon)$,

$$\int dtd^2r\langle m_i(x',\vec{r},t)m_j(x,\vec{r}=0,t=0)\rangle\exp[i(-\vec{K}\cdot\vec{r}+\omega t)] \propto [g_{ij}(x,x',\vec{K},\omega+i\varepsilon) - g_{ij}(x,x',\vec{K},\omega-i\varepsilon)],$$

in the limit $\varepsilon\to 0$. $g_{ij}(x,x',\vec{K},\omega\pm i\varepsilon)$, being responses to delta-type excitations $h_i(x)=\delta(x-x')$, can be as well regarded as magnetic Green's functions. Optical properties of the multilayered ferromagnetic structure are taken into account via the optical Green's-functions formalism. Typically applied to magneto-optical (MO) interactions in thin metal ferromagnetic structures, it has proved to be a very powerful theoretical tool, allowing to extract from the structure of the BLS spectra valuable information on the intrinsic magnetic

parameters of the investigated sample, unattainable by any other technique. In more recent papers[16] some specialized versions of this general theoretical approach have been reported.

In spite of a rapid progress, within a span of the last 5 years, of an innovative micro-Brillouin modification, typically employing externally excited coherent SW localized on individual nanoelements,[17,18] the classic "thermal magnon BLS" is still indispensable,[16,19–21] especially for the investigation of *collective* SW modes existing on the arrays of ferromagnetic elements, forming a one-dimensional (1D) or two-dimensional (2D) structure.[22–24] Not surprisingly, it is largely and successfully used to this end until now.

Although powerful and effective, the FDT implies an analysis of the magnetic system on the microscopic level, which accentuates the quantum-mechanical aspect of the problem. An alternative approach, more consistent with a purely microscopic nature of the investigated phenomena, can be developed. Moreover, it is possible to adapt, without too much difficulty, this formalism to the case of utmost importance nowadays, namely, that of nanostructured ferromagnetic films. In its main features, this technique can be reduced to the classical problem of the Brownian motion driven by the Langevin force.

The goal of this paper is theoretical description of the collective SW modes traveling in a periodic one-dimensional array of ferromagnetic stripes (magnonic modes), typically referred to as Bloch waves, and driven by a thermal "Langevin" source of magnetic field. Periodic structures of this type are also known as 1D magnonic crystals. As their closest analogs (photonic and phononic crystals) they manifest all major features characteristic of wave propagation in periodic media, such as band gaps and Brillouin zone (BZ). The latter has been confirmed experimentally in Refs. 25 and 26 (2D case). What makes their wave behavior especially interesting, from the physical point of view, is a strongly pronounced magnetically adjustable dispersion. Theoretical analysis of three-dimensional magnonic crystals reveals, not surprisingly, an even richer spectrum of wave phenomena.[27]

Our paper, focusing on the stochastic properties of thermally driven collective magnonic modes on 1D arrays of dipole coupled nanostripes is organized in the following way. At a first stage, a theoretical formalism is developed, allowing representation of such modes as an ensemble of individual harmonic oscillators interpretable in terms of independent degrees of freedom of the magnetic system subject to the low-energy Rayleigh-Jeans statistics.[28] To this end, the mathematical approach described in our earlier paper, Ref. 29, will be further generalized. The second part of this paper will be dedicated to the spatial correlation function playing a key role in various phenomena, such as Brillouin light scattering. More specifically, the correlation (coherence) length l_c for collective modes on an array of dipole coupled stripes, coupled through DDIs, will be estimated. The latter describes the spatial interval within which the phases of local point MO scatterers are sufficiently correlated which ensures the spatial coherence of the inelastically scattered light. Finally, in the last part the results obtained in the previous paragraph will be applied to the numerical estimation of the BLS angular spectrum. Special attention will be paid to the influence of the correlation (coherence) length l_c and the size of the incident optical beam d on the form of such spectra. More specifically, numerical simulations theoretically modeling the transition from incoherent inelastic scattering to coherent inelastic diffraction, experimentally studied in Ref. 30, will be performed.

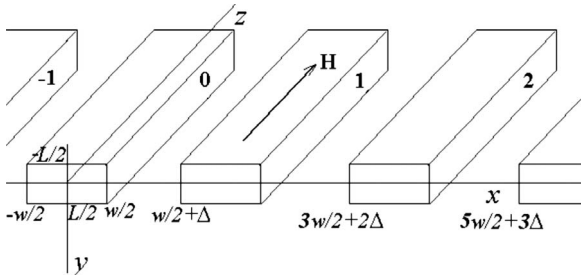

FIG. 1. Geometry of the considered array of dipole-interacting stripes.

II. THEORY

A. Basic thermodynamics

The geometry of the problem is illustrated in Fig. 1. We study collective magnetic modes existing on a periodic array of parallel infinite ferromagnetic stripes with a width w and a thickness L separated by a distance Δ. This corresponds to a spatial period equal to $T=w+\Delta$. The stripes are magnetized by an external field $H\vec{e}_z$ along their axis, i.e., along z, which means that the induced static magnetization within them $M\vec{e}_z$ is homogeneous. We limit our investigation to the case of the lowest purely dipole magnetic mode. We also assume that the aspect ratio of the stripes is small $L/w \ll 1$. In other words, we study quasi-Damon-Eshbach (DE) collective (magnonic) modes formed via dipole interactions between the oscillations localized on individual stripes. They propagate along the "x" axis and are characterized by a homogeneous distribution of the magnetization along the vertical "y" axis. The latter will make the dependence of the dipole field and the dynamic magnetization on y irrelevant which allows one to reduce the initial 2D problem to a 1D problem by averaging across the film thickness. Thus application of the highly effective approximate approach proposed in Ref. 31 and generalized for the geometry studied in Ref. 29 is fully justified.

The linearized Landau-Lifschitz equation describing thermally excited collective magnetic modes existing on an array of infinite ferromagnetic stripes can be written as

$$\frac{\partial}{\partial t} m_x(x,t) + \omega_H m_y(x,t) - \omega_M [G(x,x') \otimes m_y(x',t)] = \frac{\omega_M}{4\pi} h_y^{(th)}(x,t)$$

$$\frac{\partial}{\partial t} m_y(x,t) - \omega_H m_x(x,t) - \omega_M m_x(x,t) - \omega_M [G(x,x') \otimes m_x(x',t)] = -\frac{\omega_M}{4\pi} h_x^{(th)}(x,t) \qquad (1)$$

where $\omega_H=\gamma H$, $\omega_M=\gamma 4\pi M$, $G(x,x')\otimes m(x',t)=\int_{-\infty}^{\infty}G(x,x')m(x',t)dx'$ is the convolution integral and $G(x,x')$ is a magnetic Green's function describing DDI within each stripe, as well as between different stripes,

$$G(x,x')=\frac{1}{2\pi L}\ln\left[\frac{(x-x')^2}{L^2+(x-x')^2}\right],$$

when x and x' are within any stripes,

$$G(x,x')=0,$$

when x or/and x' is/are outside any stripe.

$\boldsymbol{h}^{(\mathrm{th})}(x,t)$ is a delta-correlated thermal Langevin force, describing thermal excitation of the magnetic modes studied,

$$\langle h_\alpha^{(th)}(x,t)h_\beta^{(th)}(x',t')\rangle=C\delta(x-x')\delta(t-t')\delta_{\alpha\beta}, \quad (2a)$$

where C is a constant, $\delta(t-t')$ is the Dirac delta function, and $\delta_{\alpha\beta}$ is the Kronecker delta with $\alpha,\beta=x,y,z$. We also assume that its mean value is zero

$$\langle h_\alpha^{(th)}(x,t)\rangle=0. \quad (2b)$$

Note that we consider $h_\alpha^{(th)}(x,t)$ to be completely real.

Introducing circular variables, corresponding to circular polarizations

$$m_\pm=m_x\pm im_y, \quad h_\pm^{(th)}=h_x^{(th)}\pm ih_y^{(th)} \quad (3)$$

allows us to simplify the system (1) in such a way that the second equation is reduced to a complex conjugate of the first one

$$\begin{cases}\dfrac{\partial}{\partial t}m(x,t)-i\left(\omega_H+\dfrac{\omega_M}{2}\right)m(x,t)-i\dfrac{\omega_M}{2}[m^*(x,t)+G(x,x')\otimes m^*(x',t)]\\ =-i\dfrac{\omega_M}{4\pi}h^{(th)}(x,t);\\ \text{c.c.}\end{cases} \quad (4)$$

Here we used the identities $m_-=m_+^*$, $h_-^{(th)}=h_+^{(th)*}$, and denoted $m\equiv m_+$, $h^{(th)}=h_+^{(th)}$. In Eq. (4) the circular polarizations of opposite directions, denoted by m and m^*, are coupled through the presence of DDIs which is unavoidable in the DE geometry and which is described by the third term on the left-hand side of Eq. (4). Physically this means, that the polarization eigenvectors are not circular, like in the case of the classic ferromagnetic resonance, but elliptic. We will deal with this later.

The solution to Eq. (4), which describes a traveling wave on a periodic structure, just as in the case considered in Ref. 29, can be represented in the form of Bloch waves,[32]

$$m_{kn}(x)=\tilde{m}_{kn}(x)\exp(ikx), \quad (5)$$

where k is a Bloch wave vector taking on continuous values, and $\tilde{m}_{kn}(x)$ is a spatially periodical function with the period T, $\tilde{m}_{kn}(x+jT)=\tilde{m}_{kn}(x)$. Here n is a mode number and j is an integer. It should be noted that in classic wave science the solution (5) is known as Floquet's theorem.[33]

Being eigenfunctions of the Hermitian integral operator

$$\lambda(k,n)m_{kn}(x)=G(x,x')\otimes m_{kn}(x') \quad (6)$$

the individual Bloch waves are mutually orthogonal

$$\int_{-\infty}^{\infty}m_{kn}(x')m_{k'n'}{}^*(x')dx'=\delta_{nn'}\delta(k-k'). \quad (7)$$

The general solution to Eq. (4) is sought in the form of a complete set of individual Bloch waves within the first Brillouin zone

$$m(x,t)=\sum_{n=1}^{\infty}\int_{-\pi/T}^{\pi/T}a_{kn}(t)\tilde{m}_{kn}(x)\exp(ikx)dk. \quad (8)$$

To obtain equations in amplitudes $a_{kn}(t)$ let us insert Eq. (8) into Eq. (4) and project both sides of the Eq. (4) on the eigenvectors, Eq. (5), taking advantage of the mutual orthogonality. Thus the problem is reduced to the solution of a standard nonhomogeneous system of spin-wave equations of motion[28]

$$\begin{cases}\dfrac{\partial}{\partial t}a_{kn}(t)+iAa_{kn}(t)+iB_{|k|n}a_{-kn}(t)^*=-i\omega_M\displaystyle\int_{-\infty}^{\infty}h^{(th)}(t,x)\tilde{m}_{kn}(x)^*\exp(-ikx)dx\\ \text{c.c.},\end{cases} \quad (9)$$

where $A=-(\omega_H+\frac{\omega_M}{2})$, $B_{|k|n}=-\frac{\omega_M}{2}-\omega_M\lambda(|k|,n)$

Since the kernel in the integral operator in Eq. (6) is symmetric its eigenvalues are real $\lambda(k,n)=\lambda(k,n)^*$. Moreover, from Eq. (6) it follows $\lambda(k,n)^*=\lambda(-k,n)$, which means that

$$\lambda(k,n)=\lambda(-k,n)=\lambda(|k|,n).$$

To obtain two separate equations in $b_{kn}(t)$ and $b_{-kn}(t)^*$, i.e., to diagonalize the system (9) we apply the Bogoliubov transformation

$$a_{kn}(t)=u_{|k|n}b_{kn}(t)+v_{|k|n}b_{-kn}(t)^*.$$

This results in an equation for normal elliptic spin-wave amplitudes,

$$\frac{\partial}{\partial t}b_{kn}(t)+(\gamma_{|k|n}+i\omega_{|k|n})b_{kn}(t)=f_{kn}(t). \tag{10a}$$

Here

$$\omega_{|k|n}=\mathrm{sgn}(A)\sqrt{A^2-B_{|k|n}^2}=-\{\omega_H(\omega_H+\omega_M)+\omega_M^2[|\lambda(|k|,n)|-\lambda^2(|k|,n)]\}^{1/2}, \tag{10b}$$

$$u_{|k|n}=\sqrt{\frac{A+\omega_{|k|n}}{2\omega_{|k|n}}},\quad v_{|k|n}=-\mathrm{sgn}(A)\frac{B_{|k|n}}{|B_{|k|n}|}\sqrt{\frac{A-\omega_{|k|n}}{2\omega_{|k|n}}}, \tag{10c}$$

$$f_{kn}(t)=-i\omega_M\{u_{|k|n}R_{kn}(t)+v_{|k|n}[R_{kn}(t)]^*\}, \tag{10d}$$

where

$$R_{kn}(t)=\int_{-\infty}^{\infty}[h^{(th)}(t,x)\tilde{m}_{kn}(x)^*\exp(-ikx)]dx, \tag{10e}$$

and following Ref. 28, have phenomenologically introduced magnetic damping $\gamma_{|k|n}$ through replacing $\omega_{|k|n}$ with $\omega_{|k|n}+i\gamma_{|k|n}$. In Eq. (10a) we have omitted the second complex conjugate equation in the system: it returns formally the frequency of the same magnon but a negative sign.

The solution of Eq. (10a) can be written as follows:

$$b_{kn}(t)=\int_0^t dt' f_{kn}(t')\exp[-(\gamma_{|k|n}+i\omega_{|k|n})(t-t')]+b_{kn}(t=0)\exp[-(\gamma_{|k|n}+i\omega_{|k|n})t]. \tag{11}$$

In the state of thermodynamic equilibrium, i.e., for $t\gg 1/\gamma_{|k|n}$, the second term disappears. Each collective mode is fully characterized by its integer index "n" and a continuous Bloch wave number k. To estimate the energy carried by each mode in the state of thermodynamic equilibrium we need to calculate the correlation function of the wave amplitudes $\langle b_{kn}(t)b_{kn}{}^*(t)\rangle$ for $t\gg 1/\gamma_{|k|n}$,

$$S_{knn}(t)=\langle b_{kn}(t)b_{kn}{}^*(t)\rangle=\int_0^t dt'\int_0^t dt''\langle f_{kn}(t')f_{kn}(t'')^*\rangle\exp[i\omega(t'-t'')]\times\exp[-\gamma_{|k|n}(2t-t'-t'')]. \tag{12}$$

According to Eq. (A6) the autocorrelation function reads

$$\langle f_{kn}(t)f_{kn}(t')^*\rangle=2C\omega_M^2\delta(t-t')(u_{|k|n}^2+v_{|k|n}^2)=2C\omega_M^2\delta(t-t')\frac{A}{\omega_{|k|n}}.$$

Here we have made use of Eqs. (9) and (10c). Thus

$$S_{knn}(t)=2C\omega_M^2\frac{A}{\omega_{|k|n}}\int_0^t dt'\exp[-2\gamma_{|k|n}t']=\frac{C\omega_M^2A}{\gamma_{|k|n}\omega_{|k|n}}[1-\exp(-2\gamma_{|k|n}t)]\underset{t\gg 1/\gamma}{\rightarrow}C\omega_M^2\frac{A}{\gamma_{|k|n}\omega_{|k|n}}.$$

In thermodynamics it is the occupation number $N_{kn}(t)$ that describes the thermal energy of the mode identified by its numbers k and n in the state of equilibrium. In other words $N_{kn}\equiv S_{knn}$ and

$$N_{kn}\equiv S_{kn}(t=\infty)=C\frac{\omega_M^2A}{2\gamma_{|k|n}\omega_{|k|n}}. \tag{13}$$

Therefore for the constant C we have

$$C=\frac{2\gamma_{|k|n}\omega_{|k|n}N_{kn}}{\omega_M^2A}. \tag{14}$$

On the other hand in the thermodynamic equilibrium the spin-wave amplitude, Eq. (13), should obey the Rayleigh-Jeans distribution,[28] thus it should have the form

$$N_{kn}=\frac{k_BT}{|\omega_{kn}|}, \tag{15}$$

therefore

$$C=\frac{2}{\omega_M^2}\frac{k_BT}{|A|}\gamma_{|k|n} \tag{16a}$$

and

$$\langle f_{kn}(t)f_{kn}(t')^*\rangle=4\gamma_{|k|n}\frac{k_BT}{|\omega_{kn}|}\delta(t-t'). \tag{16b}$$

Expression (16b) represents a modification of the FDT for the collective DE mode, in the form of a Bloch wave, propagating on an array of dipole coupled ferromagnetic stripes. Similar formulas are known since long ago as fluctuation-dissipation relation in classical Brownian motion[15] or Nyquist's noise theorem, relating the mean-square open-circuit thermal noise voltage to its resistance, in electrical engineering.[34] As one sees from this expression all peculiarities which are characteristic to the Bloch wave origin of collective excitations are hidden in the form of wave dispersion ω_{kn}. The general form of Eq. (16b) coincides with one known for spin waves in a continuous magnetic medium[28] which facilitates understanding.

B. Coherence length of thermally excited collective modes

Now we investigate the spatial correlation functions characterizing distributions of magnetization in magnetostatic

modes *at a given temporal frequency*. Knowledge of such functions is instrumental for understanding a number of significant phenomena in spin-wave physics. For example, they play a major role in mechanisms of the Brillouin light scattering by thermal magnons. To streamline our analytical calculations we employed a highly effective mathematical formalism developed in the field of Fourier optics in the 1970s.[35,36]

First, we pass from the direct temporal space "t" to the frequency space "ω" via the direct Fourier transformation. The solution of Eq. (10a) can be rewritten in the frequency domain as follows:

$$b_{kn}(\omega) = \frac{f_{kn}(\omega)}{[\gamma_{|k|n} + i(\omega_{|k|n} + \omega)]} \tag{17a}$$

with

$$b_{kn}(\omega) = \hat{\mathfrak{F}}_{t\to\omega}[b_{kn}(t)] = \lim_{\Theta\to\infty} \frac{1}{2\Theta} \int_{-\Theta}^{\Theta} dt b_{kn}(t) \exp(-i\omega t),$$

$$f_{kn}(\omega) = \hat{\mathfrak{F}}_{t\to\omega}[f_{kn}(t)]. \tag{17b}$$

Similarly, one can rewrite Eq. (2a) in the frequency domain as

$$\langle h_{\alpha}^{(th)}(x,\omega) h_{\beta}^{(th)}(x',\omega)\rangle = C\delta(x-x')\delta_{\alpha\beta}1(\omega), \tag{18}$$

where $1(\omega)$ is the Fourier transform of the Dirac delta function in Eq. (2a), as defined in the space of generalized functions.[35,36] It is equals to the constant 1 on the whole ω axis. This allows us to obtain an explicit formula for $f_{kn}(\omega)$,

$$f_{kn}(\omega) = -i\omega_M[u_{|k|n}R_{kn}(\omega) + v_{|k|n}R_{kn}(\omega)^*] \tag{19a}$$

with

$$R_{kn}(\omega) = \int_{-\infty}^{\infty} [h^{(th)}(x,\omega)\tilde{m}_{kn}(x)^* \exp(-ikx)]dx,$$

$$h^{(th)}(x,\omega) = \hat{\mathfrak{F}}_{t\to\omega}[h^{(th)}(x,t)]. \tag{19b}$$

Thus the spatial distribution of the magnetization at a given frequency can be written explicitly as

$$b(x,\omega) = \sum_{n=1}^{\infty} \int_{-\pi/T}^{\pi/T} dk b_{kn}(\omega)\tilde{m}_{kn}(x)\exp(ikx), \tag{20}$$

which allows us to define the corresponding *spatial* correlation function, averaged over the ensemble, in the following way,

$$\langle\langle b(x,\omega)b^*(x+\xi,\omega)\rangle_x\rangle = \left\langle \int_{-\infty}^{\infty} b(x,\omega)b^*(x+\xi,\omega)dx \right\rangle = \int_{-\infty}^{\infty} \langle b(x,\omega)b^*(x+\xi,\omega)\rangle dx. \tag{21}$$

Substituting Eq. (20) into Eq. (21) and taking into account the orthogonality of the eigenfunctions (7) we obtain

$$\langle\langle b(x,\omega)b^*(x+\xi,\omega)\rangle_x\rangle = \sum_n \sum_{n'} \int_{-\pi/T}^{\pi/T} dk \exp(-ik\xi) \int_{-\pi/T}^{\pi/T} dk' \langle b_{kn}(\omega)b_{k'n'}(\omega)^*\rangle \int_{-\infty}^{\infty} dx \tilde{m}_{kn}(x)\tilde{m}_{k'n'}{}^*(x+\xi)\exp(i(k-k')x). \tag{22}$$

To begin with, let us find the expression for $\langle b_{kn}(\omega)b_{k'n'}(\omega)^*\rangle$, making use of Eqs. (17a) and (A6),

$$\langle b_{kn}(\omega)b_{k'n'}(\omega)^*\rangle = \frac{\langle f_{kn}(\omega)f_{k'n'}^*(\omega)\rangle}{[\gamma_{|k|n} + i(\omega_{|k|n} + \omega)][\gamma_{|k'|n'} - i(\omega_{|k'|n'} + \omega)]} = \frac{2C\omega_M^2 A\delta(k-k')\delta_{nn'}}{\omega_{|k|n}[\gamma_{|k|n}^2 + (\omega_{|k|n} + \omega)^2]}.$$

Thus finally one obtains

$$\langle\langle b(x,\omega)b^*(x+\xi,\omega)\rangle_x\rangle = \sum_n \int_{-\pi/T}^{\pi/T} dk F_{nk}(\xi)\exp(-ik\xi)\frac{2CA\omega_M^2}{\omega_{|k|n}[\gamma_{|k|n}^2 + (\omega_{|k|n} + \omega)^2]} \tag{23a}$$

with

$$F_{nk}(\xi) = \int_{-\infty}^{\infty} \tilde{m}_{kn}(x)\tilde{m}_{kn}{}^*(x+\xi)dx. \tag{23b}$$

In other words, $F_{nk}(\xi)$ is the autocorrelation of the periodic distribution of the dynamic magnetization $\tilde{m}_{kn}(x)$.

For small magnetic damping $|V_{k_0n_0}^{(g)}|/(\gamma_{|k|n}T) \gg 1$ (the parameter $V_{k_0n_0}^{(g)}$ is explained below) two important approximations, simplifying further calculations, are justified. First, only the k vectors in the vicinity of k_0 values, that satisfies $\omega_{|k_0|n_0}+\omega=0$, contribute to the integral (23a). Therefore we may expand the eigenfrequency $\omega_{|k|n}$ in a Taylor series, in the

vicinity of k_0, keeping only the linear term $\omega_{|k|n}+\omega=\pm|V^{(g)}_{k_0n_0}|(k-k_0)$. This approximation is valid not very close to the center and the edges of the first Brillouin zone. (Near these special points $V^{(g)}_{k_0n_0}\to 0$ and the second-order term of Taylor-series expansion should be taken into account.) Second, the limits of integration can be pushed up to $(-\infty,\infty)$ which will allow us to use the method of residues. Thus we obtain

$$\langle b(x,\omega)b^*(x+\xi,\omega)\rangle = \frac{2\pi}{|V^{(g)}_{k_0n_0}(\omega)|}\frac{CA\omega_M^2}{\gamma_{|k_0|n_0}\omega_{|k_0|n_0}}F_{n_0k_0}(\xi)\exp\left[-\frac{\gamma_{k_0n_0}}{|V^{(g)}_{k_0n_0}|}|\xi|\right]\exp(-ik_0\xi), \tag{24}$$

and hence

$$|\langle b(x,\omega)b^*(x+\xi,\omega)\rangle| = \frac{2\pi}{|V^{(g)}_{k_0n_0}(\omega)|}\frac{CA\omega_M^2}{\gamma_{|k_0|n_0}\omega_{|k_0|n_0}}F_{n_0k_0}(\xi)\exp\left[-\frac{\gamma_{k_0n_0}}{|V^{(g)}_{k_0n_0}|}|\xi|\right]. \tag{25}$$

It should be noted that the indices k_0 and n_0 indicate that the corresponding values are calculated for k_0 and n_0 that satisfy $\omega_{|k_0|n_0}+\omega=0$.

Note that Eqs. (25) and (26) contain only the term of the total solution which originates from the traveling-wave part of the spin-wave excitation Green's function.[37] The term which corresponds to the source reactance was neglected as it is localized at the source and does not contribute to coherence of magnetization precession at a distance from the source.

The obtained formula allows one estimating the spin-wave coherence length l_c. We define it as the distance at which the value of correlation function is exp(1) times smaller than its original value ($\langle b(x,\omega)b^*(x+l_c,\omega)\rangle=\exp(-1)\langle b(x,\omega)b^*(x,\omega)\rangle$). Therefore the correlation length (or coherence) length for the collective mode is defined as follows:

$$l_c(k,n)=\frac{|V^{(g)}_{kn}|}{\gamma_{|k|n}}. \tag{26}$$

If the magnetic damping is small we may measure the coherence length in the number of coupled stripes j. Therefore we assume that $l_c(k,n)=jT$, we obtain

$$j=\frac{|V^{(g)}_{kn}|}{\gamma_{|k|n}T}. \tag{27}$$

The coherence length is proportional to the group velocity of the collective mode $|V^{(g)}_{kn}|=\frac{\partial\omega_{|k|n}}{\partial k}$. It may be calculated from Eq. (10b) by taking its derivative over k which gives

$$V^{(g)}_{kn}=-\frac{\omega_M\left[\frac{\omega_M}{2}+\omega_M\lambda(|k|,n)\right]}{\omega_{|k|n}}\frac{\partial\lambda(k,n)}{\partial k}. \tag{28}$$

Moreover, the derivative $\frac{\partial\lambda(k,n)}{\partial k}$ in Eq. (28) can be expressed as the following integral:

$$\frac{\partial\lambda(k,n)}{\partial k}=\int_{-\infty}^{\infty}dx\int_{-\infty}^{\infty}dx'i(x'-x)\tilde{m}_{kn}(x)G(x,x')\tilde{m}_{kn}(x')\times\exp[ik(x'-x)]dx'. \tag{29}$$

This formula will be used below in numerical calculations.

Figure 2 shows variation in the coherence length with k

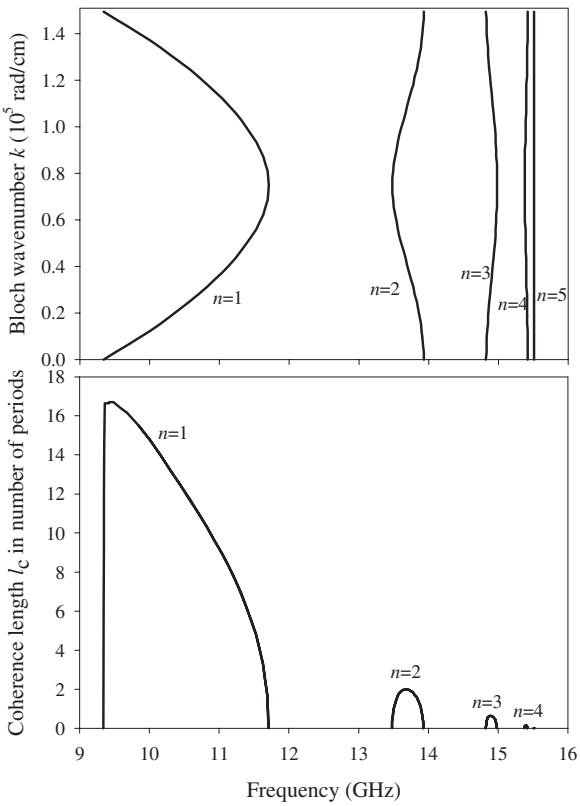

FIG. 2. Dispersion (upper panel) and coherence length of collective excitations. Parameters of calculation: stripe width: 350 nm, stripe thickness: 40 nm, stripe separation: 70 nm, saturation magnetization $4\pi M=10\,000$ G, applied field: 500 Oe, Gilbert magnetic damping constant: $\alpha=0.008$, gyromagnetic constant $\gamma/2\pi=2.82$ MHz/Oe. n in the figure denotes the mode number. The fundamental mode is $n=1$.

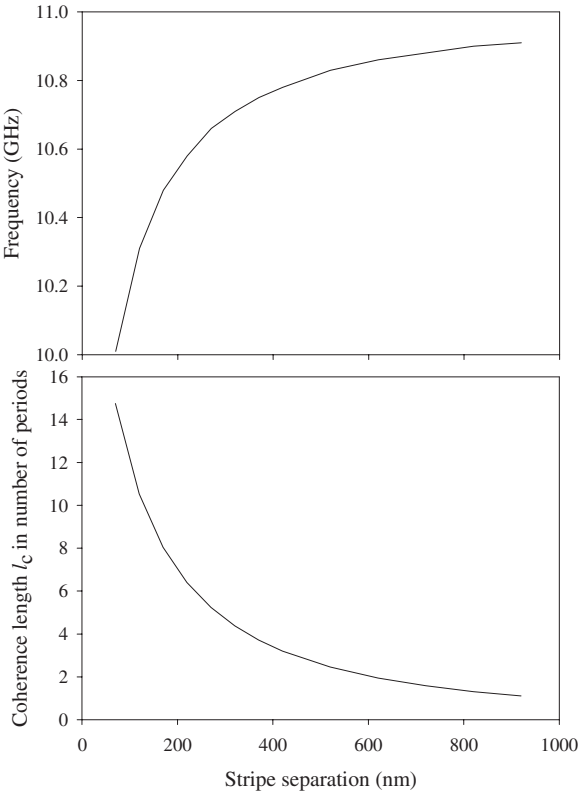

FIG. 3. Coherence length of the fundamental collective mode $n=1$ as a function of strip separation Δ for a Bloch wave number near the middle of the first Brillouin zone $k=0.17\pi/T$. Parameters of calculation are the same as for Fig. 2.

and ω. From this figure one sees that only the lowest (fundamental) $n=1$ mode of collective excitations can propagate considerable distances across the periodic structure. As one can see from the upper panel, this mode is the only mode with considerable dispersion and thus with a considerable group velocity. The latter allows this mode to cross a number of stripes during its relaxation time $1/\gamma_{|k|n}$. The coherence length drops near the middles $(k=2l\pi/T,\ l=0,1,\ldots)$ and the edges of Brillouin zones $[k=(2l+1)\pi/T]$, where Bloch waves represent standing-wave oscillations.

It is worth noticing that the decrease in the group velocity till zero toward the middle of the first BZ is very sharp and happens in a very narrow k range 0–100 rad/cm. That is why the change in the curvature near $k=0$ is not seen it the upper panel of Fig. 2. Such a narrow range of k values where the group velocity changes from the maximum to zero is a signature of strong dipole coupling of stripes in this example. Furthermore, this reflects the fact that across the BZ the dipole coupling is strongest for the zone middle where the motion of magnetization is quasihomogeneous across the whole array, as the Bloch wavelength is much larger than the structure period. With increase in the distance between stripes this k range increases and flattening of dispersion near $k=0$ becomes visible for $\Delta > w$.

Figure 3 shows variation in the coherence length with the distance between adjacent stripes Δ. This graph was calculated for the fundamental collective mode and for a Bloch number near the middle of the first BZ $(k=0.17\pi/T)$. With the increase in the distance, dipole coupling of stripes decreases. This results in a decrease in the bandwidth of the first magnonic band $(\omega_{k=\pi/T,n=1}-\omega_{k=0,n=1})$ and, consequently, in the slope of the dispersion $\omega_{k,n=1}(k)$. The former is evidenced by the upper panel of this figure which shows increase in frequency for the fundamental mode with decrease in the dipole coupling. At large separations the frequency tends to one for uncoupled stripes for which the width of the magnonic band is zero and the dispersion slope is zero too. The collective mode coherence length is zero. With the increase in the dipole coupling the collective dipole field of stripes pushes the frequency for the middle of BZ down and for the edge of the first BZ up with respect to the uncoupled stripes (see Fig. 6 in Ref. 29). The dispersion slope increases and the coherence length grows, respectively.

C. BLS intensities

Making use of Eq. (25) one can also estimate BLS intensities seen at particular angle of incidence of the laser light in the conventional (reciprocal space-resolved BLS).

The BLS spectroscopy, in its conventional nonmicro-BLS version, is based on the analysis of the intensity of the light inelastically scattered by a magnon in the inverse $k^{(s)}$ space as a function of the magnon frequency ω. The latter is related to the polarization induced through the interaction of the incident light wave and a magnetostatic mode in the following way:

$$I[k^{(s)},\omega] = \langle E[k^{(s)},\omega]E^*[k^{(s)},\omega]\rangle = \langle \hat{\mathfrak{F}}_{x\to k^{(s)}}[P(x) * P^*(x)]\rangle. \tag{30}$$

$P(x)*P^*(x)=\int_{-\infty}^{\infty}P(\xi)P^*(x+\xi)d\xi$ corresponds to the autocorrelation of the polarization with its complex conjugate, which is denoted by the symbol *. Here we do not consider the complex tensor nature of the MO interactions thus focusing on the stochastic aspect of the problem. One can find calculations of the effective cross section elsewhere (see, for example, Refs. 38 and 39). Typically, in the conventional BLS technique the divergence of the incident optical beam is small to ensure resolution in the inverse k space and the dependence of the MO cross section on the angle of incidence can be neglected. That is why we define the induced polarization, in the scalar approximation, as $P(x)=b(x,\omega)E^{(i)}(x,\omega)$.

In the particular case of a plane incident light wave characterized by an in-plane wave vector $k^{(i)}$, the Bloch wave number k in Eq. (23a) is to be replaced by $k^{(i)}+k$. Thus one obtains the classic formula[38]

$$I[k^{(s)},\omega] = \int_{-\infty}^{\infty} d\xi \langle b(x,\omega)b^*(x+\xi,\omega)\rangle \exp\{i[k^{(s)}-k^{(i)}]\xi\}, \tag{31}$$

where the ensemble average is estimated through the FDT.

Actually, however the incident optical beam is of finite size both in the direct and inverse space $E^{(i)}(x,\omega)=D(x)\exp(ik^{(i)}x)$. Here function $D(x)$ describes the distribution of the optical field in space. Thus

$$I[k^{(s)},\omega]=\int_{-\infty}^{\infty}d\xi\int_{-\infty}^{\infty}dx\langle D(x)b(x,\omega)D(x+\xi)b^{*}(x+\xi,\omega)\rangle\exp\{i[k^{(s)}-k^{(i)}]\xi\}$$

$$=\hat{\mathfrak{F}}_{\xi\to k^{(s)}-k^{(i)}}\langle\{D(x)b(x,\omega)*[D(x)b(x,\omega)]^{*}\}\rangle. \tag{32}$$

The latter means that in the inverse $q=k^{(s)}-k^{(i)}$ space the Fourier transform of $D(x)b(x,\omega)$ and its complex conjugate are multiplied. To be specific let us suppose that the light intensity within the optical spot of width d is homogeneous, i.e.,

$$D(x)=\mathrm{Rect}(2x/d),\quad \text{where}\ \ \mathrm{Rect}\left(\frac{2x}{d}\right)=\begin{cases}1 & if\ \ -\frac{d}{2}<x<\frac{d}{2}\\ 0 & if\ \ x\geq\frac{d}{2}\ \ and\ \ x\leq-\frac{d}{2}.\end{cases}$$

To begin with, we consider a particular magnetostatic mode n characterized by a particular value of the Bloch wave number k. Thus, making use of Eq. (24), the autocorrelation function in Eq. (32) can be rewritten

$$\langle D(x)b(x,\omega)*[D(x)b(x,\omega)]^{*}\rangle=\int_{-\infty}^{\infty}dx\mathrm{Rect}\left(\frac{2x}{d}\right)\mathrm{Rect}\left[\frac{2(x+\xi)}{d}\right]\langle b(x,\omega)b^{*}(x+\xi,\omega)\rangle$$

$$=H(\omega_{|k|n})F_{nk}(\xi)\exp\left[-\frac{\gamma_{kn}}{|V_{kn}^{(g)}|}|\xi|\right]\exp(-ik\xi)\left[\mathrm{Rect}\left(\frac{2\xi}{d}\right)\otimes\mathrm{Rect}\left(\frac{2\xi}{d}\right)\right].$$

To simplify notations we have put $\frac{2\pi}{|V_{kn}^{(g)}|}\frac{CA\omega_M^2}{\gamma_{|k|n}\omega_{|k|n}}=H(\omega_{|k|n})$.

In other words, in Eq. (32) the Fourier operator is applied to a product of three functions of ξ, which means that this operator returns a double convolution of the corresponding Fourier transforms,

$$\hat{\mathfrak{F}}_{\xi\to q}\left[\mathrm{Rect}\left(\frac{2\xi}{d}\right)\otimes\mathrm{Rect}\left(\frac{2\xi}{d}\right)\right]=d^{2}\ \mathrm{Sinc}^{2}(2q/d),$$

$$\hat{\mathfrak{F}}_{\xi\to q}\left\{\exp\left[-\frac{\gamma_{kn}}{|V_{kn}^{(g)}|}|\xi|\right]\exp(-ik\xi)\right\}=\frac{2\frac{\gamma_{kn}}{|V_{kn}^{(g)}|}}{(q-k)^{2}+\left[\frac{\gamma_{kn}}{|V_{kn}^{(g)}|}\right]^{2}}$$

and [see Eq. (23b)]

$$\hat{\mathfrak{F}}_{\xi\to q}[F_{nk}(\xi)]=\hat{\mathfrak{F}}_{\xi\to q}[\tilde{m}_{kn}(\xi)*\tilde{m}_{kn}(\xi)]=|\tilde{M}_{kn}(q)|^{2}$$

with $\tilde{M}_{kn}(q)=\hat{\mathfrak{F}}_{\xi\to q}[\tilde{m}_{kn}(\xi)]$ and $q=k^{(s)}-k^{(i)}$.

The periodic function $\tilde{m}_{kn}(x)$ can be regarded as a convolution of the distribution of the dynamic magnetization on a single element $s_{kn}(\xi)=\mathrm{Rect}(\frac{\xi}{T/2})\tilde{m}_{kn}(\xi)$ with a periodic comb of delta functions with T spacing, known as the Dirac comb and conventionally denoted $\mathrm{comb}(\frac{\xi}{T})$,

$$\tilde{m}_{kn}(\xi)=s_{kn}(\xi)\otimes\mathrm{comb}\left(\frac{\xi}{T}\right)$$

$$\text{with}\quad \mathrm{comb}\left(\frac{\xi}{T}\right)=\sum_{l=-\infty}^{\infty}\delta(\xi-lT).$$

Consequently, its Fourier transform is a product of the respective Fourier transforms

$$\hat{\mathfrak{F}}_{\xi\to q}[\tilde{m}_{kn}(\xi)]=S_{kn}(q)\frac{T}{2\pi}\mathrm{comb}\left(\frac{q}{\Delta q}\right)$$

and consequently

$$\hat{\mathfrak{F}}_{\xi\to q}[\tilde{m}_{kn}(\xi)*\tilde{m}_{kn}(\xi)]=\frac{T}{2\pi}\sum_{l=-\infty}^{\infty}|S_{kn}(q-l\Delta q)|^{2}\delta\left(\frac{q-l\Delta q}{\Delta q}\right).$$

Here $S_{kn}(q)=\hat{\mathfrak{F}}_{\xi\to k}[s_{kn}(\xi)]$ and $\Delta q=2\pi/T$. We have also used the well-known relation $\hat{\mathfrak{F}}_{\xi\to q}[\mathrm{comb}(\frac{\xi}{T})]=\frac{1}{\Delta q}\mathrm{comb}(\frac{q}{\Delta q})$. Thus the first convolution yields

$$|\tilde{M}_{kn}(q)|^{2}\otimes[d^{2}\ \mathrm{Sinc}^{2}(2q/d)]$$

$$=\frac{T}{2\pi}\sum_{l=-\infty}^{\infty}|S_{kn}(q-l\Delta q)|^{2}\delta\left(\frac{q-l\Delta q}{\Delta q}\right)\otimes d^{2}\ \mathrm{Sinc}^{2}(2q/d)$$

$$=\frac{Td^{2}}{2\pi}\sum_{l=-\infty}^{\infty}|S_{kn}(q-l\Delta q)|^{2}\mathrm{Sinc}^{2}\left[\frac{2(q-l\Delta q)}{d}\right].$$

A second convolution leads to the final result

$$I(q,\omega)=\frac{Td^{2}}{\pi}\frac{\gamma_{kn}}{|V_{kn}^{(g)}|}\sum_{l=-\infty}^{\infty}\int_{-\infty}^{\infty}dq'|S_{kn}(q'-l\Delta q)|^{2}$$

$$\times\mathrm{Sinc}^{2}\left[\frac{2(q'-l\Delta q)}{d}\right]\frac{1}{(q-q'-k)^{2}+\left[\frac{\gamma_{kn}}{|V_{kn}^{(g)}|}\right]^{2}}. \tag{33}$$

The square of the Sinc function, known as Fejer kernel, is a delta sequence. Thus if the width of the beam in Eq. (33) tends to the infinity $d\to\infty$, it must be replaced by a Dirac

delta function. Due to the filtering properties of the latter the integration in Eq. (33) disappears and one obtains for an infinitely wide beam

$$I(q,\omega) = I_0(k,n) \sum_{l=-\infty}^{\infty} \frac{|S_{kn}(l\Delta q)|^2}{(q - l\Delta q - k)^2 + \left(\frac{\gamma_{kn}}{|V_{kn}^{(g)}|}\right)^2},$$

$$I_0(k,n) = \frac{Td^2}{\pi} \frac{\gamma_{kn}}{|V_{kn}^{(g)}|}. \tag{34a}$$

In the inverse q space, each collective mode, due to its periodic character, will give rise to multiple responses of Lorentzian type. The weight of each peak is determined by the Fourier coefficients $|S_{kn}(l\Delta q)|^2$ while the width of each Lorentzian line depends entirely on the coherence length [see Eqs. (26) and (34a)]. This not surprising, since the coherence length $l_c(k,n)$ describes the spatial localization of coherent scattering sources.

In the general case, however each Lorentzian line is smeared by the finite angular spectrum of the incident light way, which is mathematically taken into account through a convolution of the Lorentzian function and the Fejer kernel [see Eq. (33)]. Without unnecessary loss of accuracy, the main lobe of the latter can be replaced by an equivalent rectangular function (see below), which makes the calculation straightforward, extremely rapid and reliable.

The expression (34a) can be rewritten in the domain of temporal frequencies ω,

$$I(q,\omega) = \frac{I_0(k,n)|V_{kn}^{(g)}|^2}{\gamma_{|k|n}^2 + (\omega_{|k|n} + \omega)^2} \sum_l |S_{kn}(l\Delta q)|^2. \tag{34b}$$

The BLS lines for all the responses will be centered at the frequency of resonance excitation of the mode by a thermal source $|\omega_{|k|n}| = |\omega|$. The responses will be seen at incidence angles which correspond to the transferred wave numbers

$$k + l\pi/T, \quad l = 0, \pm 1, \pm 2, \ldots \tag{35}$$

(Recall, $-\pi/T < k < \pi/T$). In which Brillouin zone $(l+1 - \pi/T + 2\pi l/T < q < \pi/T + 2\pi l/T)$ a mode gives a maximum response depends on the mode eigenprofile $\tilde{m}_{kn}(x)$ (through S_{kn}). The fundamental mode is characterized by a quasihomogeneous distribution of dynamic magnetization across the stripes and thus gives the maximum response in the first BZ. The next mode is antisymmetric and has one node across the stripe width. Its spectrum is obviously composed from odd harmonics of the structure period $2\pi l/T$, $l = \pm 1, \pm 3, \ldots$ with the maximum response in the second BZ $(l+1=2)$, etc.

A real BLS setup has a finite q resolution as it collects light from a finite range of incidence angles $\Delta\theta$. Then the corresponding range of uncertainty Δk in q (and thus in k) results in broadening of the BLS line. For simplicity we may assume that within $\Delta\theta$ intensity of all spectral components of light incident on the sample is the same. Thus in the scattered light resonance lines for eigenexcitations with frequencies ranging from $\omega_{k-\Delta k/2n}$ to $\omega_{k+\Delta k/2n}$ will be present with equal amplitude. Then in order to account for this effect one has to substitute the term $\frac{1}{\gamma_{|k|n}^2 + (\omega_{|k|n} + \omega)^2}$ in Eq. (34b) by its integral over the range of uncertainty in Δk: $U(\Delta k) = \int_{k-\Delta k/2}^{k+\Delta k/2} \frac{dk'}{\gamma_{|k'|n}^2 + (\omega_{|k'|n} + \omega)^2}$. Approximating $\omega_{k'n} = \omega_{kn} + V_{kn}^{(g)}(k' - k)$ one obtains

$$U(\Delta k) = \left[\arctan\left(\frac{\omega_{kn} + \omega + V_{kn}^{(g)}\Delta k}{\gamma_{kn}} \right) + \arctan\left(\frac{\omega + \omega_{kn} + V_{kn}^{(g)}\Delta k}{\gamma_{kn}} \right) \right] / (\gamma_{kn} V_{kn}^{(g)}). \tag{36}$$

Figure 4 shows plots of $I(q,\omega)$ in which gray scale is for the mode intensity I. It was calculated using Eq. (34a) with the term $\frac{1}{\gamma_{|k|n}^2 + (\omega_{|k|n} + \omega)^2}$ substituted by $U(k)$ as defined by Eq. (36). The uncertainty in the transferred wave number was taken 5% of the width of a Brillouin zone $2\pi/T$. The lower panel of this figure is for stripes placed far apart from one another. Dipole coupling of stripes in this geometry is small for all modes which results in a small group velocity and, consequently in a small coherence length. As a result, all the modes are practically dispersionless, as previously seen in numerous experiments.[16,19,21,40]

The middle panel is for strongly dipole coupled stripes. From this panel one clearly sees the opposite tendency: the lowest (fundamental) mode gives rise to a BLS response in the first BZ, the second one in the second BZ, and so on. Cross sections of this figure along the lines $q = 0.2 \times 10^5$ and 0.6×10^5 rad/cm are given in Fig. 5. Positions of the respective cross sections are shown in Fig. 4 by the respective vertical lines.

The middle panel is for an array of strongly dipole coupled stripes but consisting of wider stripes than for the upper panel. The width of the stripe is chosen such as it is comparable with the free propagation path in an unstructured film $\gamma V_{unstruct}^{(g)}$. From this figure one sees the BLS responses for the highest-order modes practically collapse into a continuous dispersion law for an unstructured film. This phenomenon was previously observed on uncoupled stripes.[20] Recall that the highest-order modes have a negligible width of the magnonic band and thus are not practically dipole coupled. BLS intensity for stripes at a large distance from each other is given for comparison in the lower panel.

In the last series of calculations we have estimated BLS intensity for different collection solid angles which introduce different uncertainties in the transferred wave numbers. This work was partially inspired by Ref. 30 in which BLS from a periodical array of elongated nanodots was experimentally studied. To apply our theory we treat rows of nanodots as 500-nm-wide stripes of infinite length with 250 nm interstripe separation. Our calculation shows that these effective stripes are efficiently dipole coupled. The collective mode dispersion as seen by BLS with a small collection solid angle is shown in Fig. 6, upper right panel. The upper left panel demonstrate the same calculation for a collection angle which corresponds to $\frac{1}{2}$ of the width of the BZ for this quasicrystal lattice $(\Delta q = \pi/T)$. One sees a broad intensity peak for the main mode and much narrower peaks for the higher-order modes. Cross sections of the 2D plots in the upper panels along the edge of the first BZ $q = \pi/T$ are shown in the lower panels.

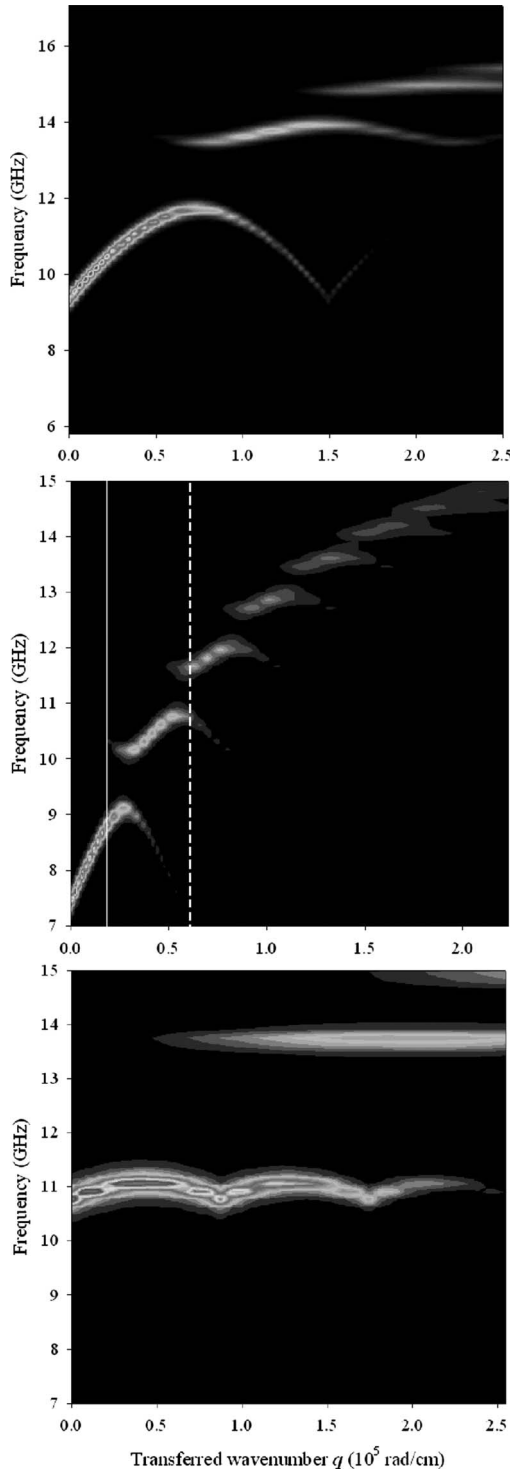

FIG. 4. "Intensities" of collective modes as seen by Brillouin light scattering technique for different stripe widths w and separations d. Upper panel: $w=350$ nm and $\Delta=70$ nm. Middle panel: $w=1050$ nm and $\Delta=70$ nm. Lower panel: $w=\Delta=350$ nm. Laser beam width $d=\infty$. Brighter gradations of gray correspond to larger intensity. The other parameters of calculation are the same as in Fig. 2. The Gilbert damping constant entering the expression for magnetic damping $\gamma_{nk}=\alpha\omega_{nk}$ is as for permalloy $\alpha=0.008$. (The spot structure seen in the data is an artefact of presentation of calculated data by the plotting software used. It is connected with discreetness of input data for the software.)

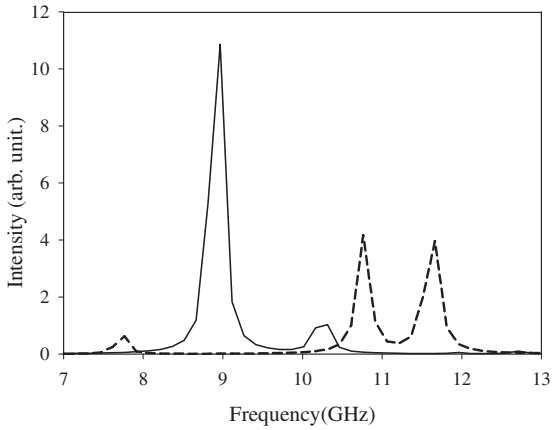

FIG. 5. Cross sections of the 2D plot in Fig. 4, middle panel, along the lines $q=0.2\times10^5$ rad/cm (solid line) and 0.6×10^5 rad/cm (dashed line). Positions of the respective cross sections are shown in Fig. 4 by the respective vertical lines.

The lowest collective mode gives rise to the broadest intensity peak for $\Delta q=\pi/T$. This mode is characterized by the largest correlation length due to the largest group velocity (dispersion slope). Furthermore, it is characterized by the largest frequency band (magnonic band). The closest higher-order mode forms a much smaller magnonic band. Furthermore, it is almost dispersionless which results in a much smaller correlation length for this mode. Thus, in our calculation decreasing the collection angle for the case of the mode with a large correlation length results in a considerable narrowing of the BLS peak and decrease in its intensity. On the contrary, the first higher-order mode does not exhibit a considerable change in the peak width with decrease in the collection angle. Importantly, the peak intensity decreases considerably similar to the lowest-order mode.

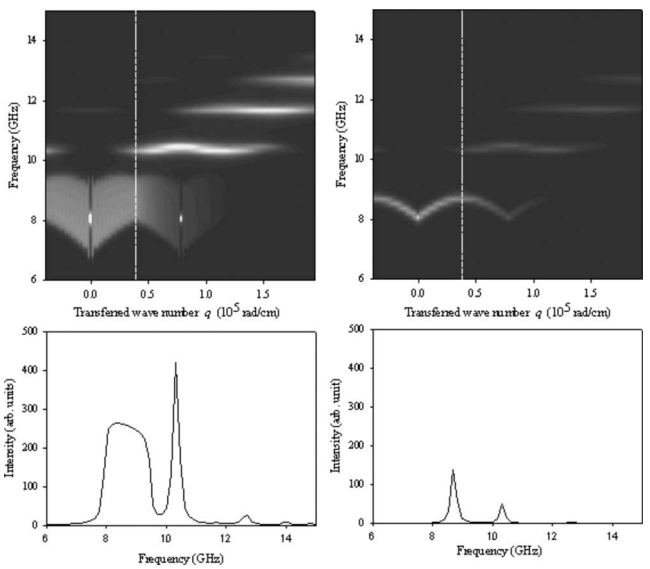

FIG. 6. Intensities for different collecting lens apertures. Left panels: the lens collects the light from the solid angle corresponding to $\frac{1}{2}$ of the Brillouin zone. Right panel: 1/10 of the Brillouin zone. Upper panels: intensities. Lower panels: cross sections of the upper panels along the edge of the first Brillouin zone π/T. Brightness scale is the same for both upper panels.

Thus the behavior of the peak amplitude is in good agreement with Ref. 30, which is not the case for the evolution of the peak width. We suggest the following explanation for this disagreement. First, the array in Ref. 30 is a set of nanodots. The nanodots as 2D objects are characterized by a much richer spectrum of eigenoscillations with broader frequency bands than the quasi-1D nanostripes (see, e.g., Ref. 41). Therefore, increasing the collection angle results in collecting a BLS response from a larger number of eigenexcitations thus from a larger frequency band. If the dynamics is driven by a spectrally narrow source, like a microwave generator, the increase in the collection angle does not result in a change in the peak width, as the peak width is given by the linewidth of the microwave generator, which is negligible, and the instrumental linewidth of the Sandercock interferometer.

One has to note that a periodic stripe array represents a diffraction lattice for the incident laser light. In particular, the authors of Ref. 30 note that the diffracted beams originating from the patterned sample are clearly visible to the naked eye. Thus multiple maxima of diffraction of the laser light in reflection can be formed. This scattering is "elastic" as the frequency of light is conserved. In the backscattering geometry of BLS experiment the light which has elastically scattered into all orders of diffraction n_d can then scatter from all harmonics $\tilde{m}_{knl}$ of the collective modes. This modifies the resonance scattering condition (35). The more precise condition for resonance scattering of the light reads,

$$q = k + 2\pi(l - n_d)/T. \tag{37}$$

Following this condition inelastically scattered light collected at an incidence angle $\theta = \arcsin\{[k + 2\pi(l - n_d)/T](\lambda_{las}/4\pi)\}$ will represent a combination of responses from all orders of elastic diffraction n_d and of inelastic scattering from all harmonics l of the collective modes which satisfy the above condition for θ. This reflects the double-scattering nature of this contribution: at the first stage, the light is diffracted elastically by the relief lattice and after this the second MO scattering occurs. In the present calculation for simplicity reasons we do not account for this effect, as for a *highly pronounced* collective behavior the stripes should be closely spaced (<200 nm apart). This means that the elastic scattering is dominated by near-field mechanisms, which makes it relatively inefficient.

As a final note for this section we now discuss validity of our theory of the magneto-optical interaction. Its obvious limitation is its scalar character. An important consequence of this is a loss of the so-called Stokes-anti-Stokes asymmetry of BLS peaks for the Damon-Eschbach wave.[42,43] This effect represents a difference in the BLS amplitudes for the positive and negative frequencies. This difference is seen, e.g., in Fig. 5 of Ref. 22.

One can separate two contributions to this effect. One is connected to the fact that the magneto-optical interaction is described by a *tensor* magnitude: the magneto-optical tensor. Its action on the circularly polarized *vector* amplitude of dynamic magnetization depends on the direction of the transferred wave number. An interested reader can find an extensive discussion concerning this point in Ref. 44. As we do not include the magneto-optical tensor into the derivation of Eq. (34a), and treat the magneto-optical interaction as a scalar, we loose this contribution to the Stokes/anti-Stokes asymmetry.

The second contribution to the Stokes-anti-Stokes asymmetry appears in experiments for larger wave numbers such as kL is on order of 1. This contribution is related to the surface character of the Damon-Eshbach wave and to the skin depth law valid for the optical field in the sample. In simple words, the thickness profile of the Damon-Eshbach wave propagating along the film surface facing the incident optical beam has a larger overlap integral with the optical field than the mode profile for the wave localized at the second film surface. This contribution is not included in our theory either, since to include it one should have treated the magnetization dynamics in the stripes thickness resolved, as it was done in a recent paper.[45] In the present paper, to keep the results simple we use the simple quasi-one-dimensional description of the magnetization dynamics (see discussion in the beginning of Sec. II A). This description is valid for $kL < 0.5$.[46] For these wave numbers the Damon-Eshbach wave localization at the film surfaces is not important and is neglected from very beginning of the derivation.

III. CONCLUSION

Formation of collective magnetostatic modes via dipolar coupling between individual elements is the main physical mechanism underlying magnonic wave phenomena in periodic ferromagnetic structures. In the present paper, this fundamental problem has been addressed for the case of thermally driven MSW on a one-dimensional array of magnetic stripes.

It has been shown that partially phase-correlated oscillations localized on individual stripes can be regarded as an ensemble of individual harmonic oscillators interpretable in terms of independent degrees of freedom of the magnetic system subject to the low-energy Rayleigh-Jeans statistics.

Further theoretical analysis, based on the spatial correlation approach, has revealed the importance of the parameter l_c known as correlation or coherence length of a Bloch mode, driven by a thermal "Langevin magnetic source." The latter describes the number of dipole coupled individual oscillations localized on individual stripes, whose phases are effectively correlated according to the Bloch wave number q, imposed by the collective mode.

Numerical simulations of the BLS spectra, based on this approach, have shown that the nth Bloch mode in strongly coupled stripes contributes mainly to the scattering in the nth Brillouin zone. This is not the case for weakly coupled stripes with higher values of interwire spacing. In such geometries l_c can decrease drastically and, as a result, for example, the fundamental Bloch mode will contribute significantly to the scattering in several lowest Brillouin zones. Our calculations have also confirmed numerically the noncoherent wide-angle character of the BLS, demonstrated experimentally in Ref. 30.

ACKNOWLEDGMENTS

Support by the Australian Research Council and LPMTP,

Université Paris-13 is gratefully acknowledged.

APPENDIX

Let us try to estimate the correlation function, describing the Langevin force exciting elliptically polarized Bloch modes, which is given below. This expression will be extremely useful in the context of the main text of the paper

$$\begin{aligned}\langle f_{kn}(t)f_{k'n'}(t')^*\rangle = \omega_M^2[&u_{|k|n}u_{|k'|n'}\langle R_{kn}(t)R_{k'n'}(t')^*\rangle \\ &+ v_{|k|n}v_{|k'|n'}\langle R_{kn}(t)^*R_{k'n'}(t')\rangle \\ &+ u_{|k|n}v_{|k'|n'}\langle R_{kn}(t)R_{k'n'}(t')\rangle \\ &+ v_{|k|n}u_{|k'|n'}\langle R_{kn}(t)^*R_{k'n'}(t')^*\rangle].\end{aligned} \tag{A1}$$

Each particular correlation function, out of four, can be evaluated independently. We will begin with the first and the third.

$$\begin{aligned}\langle R_{kn}(t)R_{k'n'}(t')^*\rangle = &\int_{-\infty}^{\infty}\int_{-\infty}^{\infty} dxdx' m_{kn}{}^*(x)m_{k'n'}(x') \\ &\times\langle h^{(th)}(x,t)h^{(th)*}(x',t')\rangle,\end{aligned} \tag{A2a}$$

$$\begin{aligned}\langle R_{kn}(t)R_{k'n'}(t')\rangle = &\int_{-\infty}^{\infty}\int_{-\infty}^{\infty} dxdx' m_{kn}{}^*(x)m_{k'n'}{}^*(x') \\ &\times\langle h^{(th)}(x,t)h^{(th)}(x',t')\rangle.\end{aligned} \tag{A2b}$$

In Eq. (A2) a key role is played by the averaged expressions within the brackets,

$$\begin{aligned}\langle h^{(th)}(x,t)h^{(th)*}(x',t')\rangle &= \langle[h_x^{(th)}(x,t)+ih_y^{(th)}(x,t)][h_x^{(th)}(x',t')-ih_y^{(th)}(x',t')]\rangle \\ &= \langle h_x^{(th)}(x,t)h_x^{(th)}(x',t')\rangle + \langle h_y^{(th)}(x,t)h_y^{(th)}(x',t')\rangle + i\langle h_x^{(th)}(x,t)h_y^{(th)}(x',t')\rangle + \langle h_y^{(th)}(x,t)h_x^{(th)}(x',t')\rangle,\end{aligned} \tag{A3a}$$

$$\begin{aligned}\langle h^{(th)}(x,t)h^{(th)}(x',t')\rangle &= \langle[h_x^{(th)}(x,t)+ih_y^{(th)}(x,t)][h_x^{(th)}(x',t')+ih_y^{(th)}(x',t')]\rangle \\ &= \langle h_x^{(th)}(x,t)h_x^{(th)}(x',t')\rangle - \langle h_y^{(th)}(x,t)h_y^{(th)}(x',t')\rangle + i\langle h_x^{(th)}(x,t)h_y^{(th)}(x',t')\rangle + \langle h_y^{(th)}(x,t)h_x^{(th)}(x',t')\rangle.\end{aligned} \tag{A3b}$$

Here we used the expression of the Langevin force in circular polarizations $h(x,t)=h_x(x,t)+ih_y(x,t)$ [see Eq. (3)]. It should be reminded that the Cartesian components of the thermal magnetic field are purely real. Making use of Eq. (2) one can rewrite Eq. (A3) as

$$\langle h^{(th)}(x,t)h^{(th)*}(x',t')\rangle = 2C\delta(x-x')\delta(t-t'), \tag{A4a}$$

$$\langle h^{(th)}(x,t)h^{(th)}(x',t')\rangle = 0. \tag{A4b}$$

Moreover

$$\langle h^{(th)*}(x,t)h^{(th)}(x',t')\rangle = \langle h^{(th)}(x,t)h^{(th)*}(x',t')\rangle^* = 2C\delta(x-x')\delta(t-t'), \tag{A4c}$$

$$\langle h^{(th)*}(x,t)h^{(th)*}(x',t')\rangle = \langle h^{(th)}(x,t)h^{(th)}(x',t')\rangle^* = 0. \tag{A4d}$$

Inserting Eqs. (A4a) and (A4b) in Eqs. (A2a) and (A2b), respectively, one obtains

$$\begin{aligned}\langle R_{kn}(t)R_{k'n'}(t')^*\rangle &= 2C\omega_M^2\int_{-\infty}^{\infty}\int_{-\infty}^{\infty} dxdx' m_{kn}{}^*(x)m_{k'n'}(x')\delta(x-x')\delta(t-t') \\ &= 2C\omega_M^2\delta(t-t')\int_{-\infty}^{\infty} dx m_{kn}{}^*(x)m_{k'n'}(x) = 2C\omega_M^2\delta(t-t')\delta(k-k')\delta_{nn'},\end{aligned} \tag{A5a}$$

$$\langle R_{kn}(t)R_{k'n'}(t')\rangle = 0. \tag{A5b}$$

Similarly

$$\langle R_{kn}(t)^*R_{k'n'}(t')\rangle = \langle R_{kn}(t)R_{k'n'}(t')^*\rangle^* = 2C\omega_M^2\delta(t-t')\delta(k-k')\delta_{nn'}, \tag{A5c}$$

$$\langle R_{kn}{}^*(t)R_{k'n'}{}^*(t')\rangle = \langle R_{kn}(t)R_{k'n'}(t')\rangle^* = 0. \tag{A5d}$$

Inserting Eqs. (A5a)–(A5d) into Eq. (A1) and taking into account the orthonormality of the eigenfunctions Eq. (7) one finally obtains

$$\langle f_{kn}(t) f_{k'n'}(t')^* \rangle = [u_{|k|n} u_{|k'|n'} 2C\omega_M^2 \delta(t-t')\delta(k-k')\delta_{nn'} + v_{|k|n} v_{|k'|n'} 2C\omega_M^2 \delta(t-t')\delta(k-k')\delta_{nn'}]$$

$$= 2C\omega_M^2 \delta(t-t')\delta(k-k')\delta_{nn'}(u_{|k|n}^2 + v_{|k|n}^2) = \frac{2AC\omega_M^2}{\omega_{|k|n}} \delta(t-t')\delta(k-k')\delta_{nn'}. \quad \text{(A6)}$$

Similar calculations are applicable for the correlation function in the frequency domain

$$\langle f_{kn}(\omega) f_{k'n'}^*(\omega) \rangle = \omega_M^2 \Bigg\{ u_{|k|n} u_{|k'|n'} \int_{-\infty}^{\infty}\int_{-\infty}^{\infty} m_{kn}(x)^* m_{k'n'}(x') \langle [h_x^{(th)}(x,\omega) + i h_y^{(th)}(x,\omega)][h_x^{(th)}(x',\omega) - i h_y^{(th)}(x',\omega)] \rangle dx dx'$$

$$+ v_{|k|n} v_{|k'|n'} \int_{-\infty}^{\infty}\int_{-\infty}^{\infty} m_{kn}(x) m_{k'n'}(x')^* \langle [h_x^{(th)}(x,\omega) - i h_y^{(th)}(x,\omega)][h_x^{(th)}(x',\omega) + i h_y^{(th)}(x',\omega)] \rangle dx dx'$$

$$+ u_{|k|n} v_{|k'|n'} \int_{-\infty}^{\infty}\int_{-\infty}^{\infty} m_{kn}(x)^* m_{k'n'}(x')^* \langle [h_x^{(th)}(x,\omega) + i h_y^{(th)}(x,\omega)][h_x^{(th)}(x',\omega) + i h_y^{(th)}(x',\omega)] \rangle dx dx'$$

$$+ v_{|k|n} u_{|k'|n'} \int_{-\infty}^{\infty}\int_{-\infty}^{\infty} m_{kn}(x) m_{k'n'}(x') \langle [h_x^{(th)}(x,\omega) - i h_y^{(th)}(x,\omega)][h_x^{(th)}(x',\omega) - i h_y^{(th)}(x',\omega)] \rangle dx dx' \Bigg\}$$

which leads finally to

$$\langle f_{kn}(\omega) f_{k'n'}^*(\omega) \rangle = \frac{2AC\omega_M^2}{\omega_{|k|n}} 1(\omega)\delta(k-k')\delta_{nn'}. \quad \text{(A7)}$$

[1] G. Binasch, P. Grünberg, F. Saurenbach, and W. Zinn, Phys. Rev. B **39**, 4828 (1989).

[2] M. N. Baibich, J. M. Broto, A. Fert, F. Nguyen van Dau, F. Petroff, P. Etienne, A. Creuzot, A. Friedrich, and J. Chazeles, Phys. Rev. Lett. **61**, 2472 (1988).

[3] R. L. Stamps and B. Hillebrands, Appl. Phys. Lett. **75**, 1143 (1999).

[4] Y. Acremann, C. H. Back, M. Buess, O. Portmann, A. Vaterlaus, D. Pescia, and H. Melchior, Science **290**, 492 (2000).

[5] A. I. Akhiezer, V. G. Baryakhtar, and S. V. Peletminskii, *Spin-Waves* (North-Holland, Amsterdam, 1968).

[6] D. D. Stancil, *Theory of Magnetostatic Waves* (Springer-Verlag, Berlin, 1993).

[7] B. A. Kalinikos, in *Linear and Nonlinear Spin Waves in Magnetic Films and Superlattices*, edited by M. G. Cottam (World Scientific, Singapore, 1994), pp. 90–156.

[8] A. S. Borovik-Romanov, V. G. Zhotikov, N. M. Kreines, and A. A. Pankov, JETP Lett. **23**, 705 (1976).

[9] W. Wettling, W. Jantz, and C. E. Patton, J. Appl. Phys. **50**, 2030 (1979).

[10] J. R. Sandercock, in *Light Scattering in Solids*, edited by M. Cardona and G. Güntherodt (Springer-Verlag, Berlin, 1982), Vol. III, p. 173.

[11] B. Hillebrands, in *Novel Techniques for Characterizing Magnetic Materials*, edited by Y. Zhu (Springer, New York, 2005).

[12] R. E. Camley and D. L. Mills, Phys. Rev. B **18**, 4821 (1978).

[13] M. G. Cottam, J. Phys. C **12**, 1709 (1979).

[14] R. E. Camley, T. S. Rahman, and D. L. Mills, Phys. Rev. B **23**, 1226 (1981).

[15] http://www.phys.ens.fr/cours/college-de-france/1977-78/1977-78.htm, lectures on Theoretical Physics given at the College de France by C. Cohen-Tannoudji.

[16] Y. Roussigné, S. M. Cherif, C. Dugautier, and P. Moch, Phys. Rev. B **63**, 134429 (2001).

[17] V. E. Demidov, S. O. Demokritov, K. Rott, P. Krzysteczko, and G. Reiss, Appl. Phys. Lett. **92**, 232503 (2008).

[18] V. E. Demidov, S. O. Demokritov, K. Rott, P. Krzysteczko, and G. Reiss, Phys. Rev. B **77**, 064406 (2008).

[19] C. Mathieu, J. Jorzick, A. Frank, S. O. Demokritov, A. N. Slavin, B. Hillebrands, B. Bartenlian, C. Chappert, D. Decanini, F. Rousseaux, and E. Cambril, Phys. Rev. Lett. **81**, 3968 (1998).

[20] J. Jorzick, S. O. Demokritov, C. Mathieu, B. Hillebrands, B. Bartenlian, C. Chappert, F. Rousseaux, and A. N. Slavin, Phys. Rev. B **60**, 15194 (1999).

[21] G. Gubbiotti, P. Candeloro, L. Businaro, E. Di Fabrizio, A. Gerardino, R. Ziveri, M. Conti, and G. Carlotti, J. Appl. Phys. **93**, 7595 (2003).

[22] G. Gubbiotti, S. Tacchi, G. Carlotti, P. Vavassori, N. Singh, S. Goolaup, A. O. Adeyeye, A. Stashkevich, and M. Kostylev, Phys. Rev. B **72**, 224413 (2005).

[23] Z. K. Wang, H. S. Lim, H. Y. Liu, S. C. Ng, M. H. Kuok, L. L. Tay, D. J. Lockwood, M. G. Cottam, K. L. Hobbs, P. R. Larson, J. C. Keay, G. D. Lian, and M. B. Johnson, Phys. Rev. Lett. **94**, 137208 (2005).

[24] Z. K. Wang, V. L. Zhang, H. S. Lim, S. C. Ng, M. H. Kuok, S. Jain, and A. O. Adeyeye, Appl. Phys. Lett. **94**, 083112 (2009).

[25] S. A. Nikitov, Ph. Tailhades, and C. S. Tsai, J. Magn. Magn. Mater. **236**, 320 (2001).

[26] S. L. Vysotskii, S. A. Nikitov, and Yu. A. Filimonov, Sov. Phys. JETP **101**, 547 (2005).

[27] M. Krawczyk and H. Puszkarski, Phys. Rev. B **77**, 054437 (2008).

[28] V. S. L'vov, *Wave Turbulence Under Parametric Excitation* (Springer-Verlag, Berlin, 1994).

[29] M. P. Kostylev, A. A. Stashkevich, and N. A. Sergeeva, Phys. Rev. B **69**, 064408 (2004).

[30] M. Grimsditch, F. Y. Fradin, Y. Ji, A. Hoffmann, R. E. Camley, V. Metlushko, and V. Novosad, Phys. Rev. Lett. **96**, 047401

(2006).
[31] K. Yu. Guslienko, S. O. Demokritov, B. Hillebrands, and A. N. Slavin, Phys. Rev. B **66**, 132402 (2002).
[32] C. Kittel, *Quantum Theory of Solids* (Wiley, New York, London, 1963).
[33] P. M. Morse and H. Feshbach, *Methods of Theoretical Physics, Part 1* (McGraw-Hill, New York, 1953).
[34] L. D. Landau and E. M. Lifshitz, *Electrodynamics of Continuous Media (Course of Theoretical Physics)* (Pergamon, London, Paris, 1959).
[35] L. M. Soroko, *Holography and Coherent Optics* (Plenum, New York, 1980).
[36] A. Papoulis, *Systems and Transforms with Applications in Optics* (Krieger, Malabar, Florida, 1981).
[37] T. Schneider, A. A. Serga, T. Neumann, B. Hillebrands, and M. P. Kostylev, Phys. Rev. B **77**, 214411 (2008).
[38] M. G. Cottam and D. J. Lockwood, *Light Scattering in Magnetic Solids* (Wiley, New York, Chichester, Brisbane, Toronto, Singapore, 1986).
[39] I. V. Rojdestvenski, M. G. Cottam, and A. N. Slavin, Phys. Rev. B **48**, 12768 (1993).
[40] N. A. Sergeeva, S. M. Cherif, A. A. Stashkevich, M. P. Kostylev, and J. Ben Youssef, J. Magn. Magn. Mater. **288**, 250 (2005).
[41] C. Bayer, J. Jorzick, S. O. Demokritov, A. N. Slavin, K. Y. Guslienko, D. V. Berkov, N. L. Gorn, M. P. Kostylev, and B. Hillebrands, in *Spin Dynamics in Confined Magnetic Structures III*, Topics in Applied Physics Vol. 101, edited by B. Hillebrands and K. Ounadjela (Springer, Berlin, 2006), pp. 57–103.
[42] R. E. Camley, P. Grunberg, and C. M. Mayr, Phys. Rev. B **26**, 2609 (1982).
[43] R. Zivieri, P. Vavassori, L. Giovannini, F. Nizzoli, E. E. Fullerton, M. Grimsditch, and V. Metlushko, Phys. Rev. B **65**, 165406 (2002).
[44] A. Stashkevich *et al.*, Phys. Rev. B **80**, 144406 (2009).
[45] M. Kostylev, P. Schrader, R. L. Stamps, G. Gubbiotti, G. Carlotti, A. O. Adeyeye, S. Goolaup, and N. Singh, Appl. Phys. Lett. **92**, 132504 (2008).
[46] M. P. Kostylev and N. A. Sergeeva, in *Magnetic Properties of Laterally Confined Nanometric Structures*, edited by G. Gubbiotti (Transworld Research Network, Kerala, India, 2006), pp. 183–207.